A Textile-Based Approach to Wearable Haptic Devices

Barclay Jumet, *Student Member, IEEE*, Zane A. Zook, *Student Member, IEEE*, Doris Xu, Nathaniel Fino, Anoop Rajappan, Mark W. Schara, Jeffrey Berning, Nicolas Escobar, Marcia K. O'Malley, *Fellow, IEEE*, Daniel J. Preston, *Member, IEEE*

Abstract—Our sense of touch offers a useful mode of communication through haptics that can augment the oftencrowded visual and auditory pathways, but haptic devices have yet to be fully integrated into garments and other soft wearables in a way that maintains the compliance and comfort of everyday clothing, resulting in a barrier to widespread adoption. We introduce a haptic device—a squeeze band—made entirely from textiles. This textile-based device is actuated by pressurized air, and its force-pressure response can be tailored in a controllable manner by altering the geometry of internal inflatable regions within the device during a rapid and inexpensive process of fabrication. We describe this fabrication and characterize six different squeeze bands that exemplify the highly tunable nature of our textile-based approach to wearable haptic devices.

I. INTRODUCTION

Efficient and effective communication in our increasingly attention-demanding environments requires communicative pathways that can interface well with each other and within our everyday lives. Humans often rely on visual and auditory signals in their day-to-day activities, and information can be lost in the "noise" of those encumbered pathways of communication. Haptic cues, delivered through kinesthetic and tactile signals, serve as a proven method for adding tobut not further cluttering—the typical ways in which humans communicate, not only with each other but also with computers, machines, and robots [1]. Moreover, people with clinically impeded pathways of communication can oftentimes benefit from alternative modes of communication that align with their particular needs [2]. Haptic devices are thus well suited to supplement our often overloaded or impaired visual and auditory pathways, especially in augmented and virtual realities [3], navigation of relatively complex environments [4], and human-robot interaction (HRI) [5], [6].

A recent focus of research entails the wearable aspect of haptic devices [7], [8]. These devices generate tactile cues to stimulate mechanoreceptors in the skin that respond to pressure and touch [1]. Lately, research has centered on the use of rigid electromechanical devices anchored by a soft or compliant material to ground the forces from the device to the user's body. Rigid haptic devices have been integrated into items that emulate often-worn adornments, including

This research is supported by the National Science Foundation (NSF) Graduate Research Fellowship under Grant No. 1842494 and by NSF CMMI-1830146. Any opinions, findings, and conclusions or recommendations expressed in this material are those of the authors and do not necessarily reflect the views of the NSF. B. Jumet, Z. A. Zook, and J. Berning acknowledge support from the NSF Graduate Research Fellowship.

B. Jumet, Z. A. Zook, D. Xu, N. Fino, A. Rajappan, M. W. Schara, J. Berning, N. Escobar, M. K. O'Malley, and D. J. Preston* are with Rice University, 6100 Main St., Houston, TX 77005 USA. (*corresponding author e-mail: djp@rice.edu).

wristbands (e.g., bracelets) [5], [9], [10], armbands (and sleeves), gloves [11], and jackets or vests [12], [13].

Going a step further, a burgeoning research direction for wearable haptics involves the development or employment of fully soft haptic devices. Recent advances leverage silicone or similar elastomers, as seen in elastomeric reed-based vibrotactors [14], microfluidic elastomeric Braille displays based on combustion sparked by liquid metal electrodes [15], and arrays of dielectric elastomeric actuators (DEAs) [16], [17]. Squeeze and stretch cues have been demonstrated in "fluidic fabric muscle sheets" that employ elastic tubing integrated into a textile sheet [18], [19]. Other fluidic approaches with soft materials typically include inextensible yet compliant two-dimensional (2D) materials, such as sheets of polymers [20]–[22].

In this work, we introduce an approach for wearable haptic devices made entirely from heat-sealable textiles (HSTs). The squeeze band shown in this work is composed of two sheets of HST and an intermediate patterned non-stick sheet. The HST sheets are hermetically heat sealed together, and the patterned non-stick sheet between the HST sheets creates localized, predefined unbonded regions. These internal unbonded regions then act as (i) channels through which fluid can be routed or (ii) pouches that inflate upon pressurization. Due to the inextensibility of the HSTs, inflation of the pouches causes contraction tangential to the surface of the device, in an architecture known as a pouch motor [23], [24]. We extend the use of a pouch motor by adapting it to leverage the concept of Laplace pressure [25] to deliver the squeeze cue, which sets this work apart from a prior demonstration in which a textilebased device applied localized compression [26]. When the device is wrapped securely around a user's wrist (or any appendage), this tangential (i.e., circumferential) contraction induces an evenly distributed Laplace pressure felt by the user as a radial squeeze (Fig. 1), in this manner differing from blood pressure cuffs and other similar devices that rely on the expansion of a bladder [22], [27]-[30] rather than the contraction of a band or sleeve shown herein.

Fully textile squeeze band



Figure 1. Operational principle of the textile haptic squeeze band: a pressure supply inflates pouches within the band, causing it to contract circumferentially and delivering a squeeze cue to the wearer.

This textile-based squeeze band is constructed from low-cost and compliant fabrics that enable facile 2D fabrication (e.g., laser cutting or vinyl cutting followed by heat pressing or ironing, with the potential for roll-to-roll manufacturing at scale) [31]. The use of air as a function medium [32] ensures a lightweight and washable device that can be used in a variety of environments and applications.

II. OVERVIEW AND FABRICATION OF HST-BASED DEVICES

Textiles are the quintessential material for wearables due to their ubiquitous use in clothing [33]. Beyond clothing, textiles are common in automobiles, furniture, backpacks and bags, beds, blankets, toys, and a host of other everyday items. HSTs in particular are already used in mass manufacturing methods, are commercially available and inexpensive, and offer the capability for "do-it-yourself" (DIY) solutions and at-home fabrication. The approach outlined in this paper benefits from (i) simple fabrication (Fig. 2) compared to the current state of the art, (ii) highly tunable force output characteristics, and (iii) characteristics of force (from 1.7 N in our weakest squeeze band at 50 kPa to 67 N in our strongest squeeze band at 100 kPa) and latency (~150 ms rise time of applied force) that are comparable to other compliant wearable haptic devices (we note that prior work indicates squeeze forces of less than 10 N have been sufficient for haptic communication [34]). These merits are compounded by the advantages of the lightweight, conforming, and comfortable properties that textile-based devices in general inherently provide over their rigid counterparts, amounting to a haptically

capable device that is able to be integrated into our clothing and other aspects of everyday life.

A. Materials

We used a nylon taffeta textile (FHST, Seattle Fabrics) with a thermoplastic polyurethane (TPU) backing for all HST layers, although any HSTs (i.e., any composite textile-thermoplastic sheets) could be employed using the principles described in this work. The non-stick layers are made from an adhesive-backed paper (DL8511FS, Packzon). The adhesive backing allowed for single-step cutting of all features during fabrication. Pneumatic pressure was supplied through a Luer lock dispensing tip (JG13-0.5HPX, Jensen Global), although a variety of fully soft attachment mechanisms are available [31]. The Luer lock dispensing tip is permanently sealed to the device with epoxy (Plastic Bonder 50139, JB Weld). Lastly, adhesive-backed hook and loop fastener (94985K35, McMaster-Carr) facilitates easy donning and doffing of the squeeze band.

B. Fabrication

The squeeze band can be manufactured through a variety of 2D manufacturing processes; we employed a vinyl cutter (Maker 3, Cricut) and heat press (DK20SP, Digital Knight) for fabrication (**Fig. 2a**). The internal geometries of the pouches and pathways for airflow in the non-stick layer (i.e., the adhesive-backed paper) are cut with a shallow first pass then followed with a second pass using a deeper cut to define the squeeze band and alignment tabs. The remaining weeded layers are aligned and thermally bonded at 200° C and 345 kPa

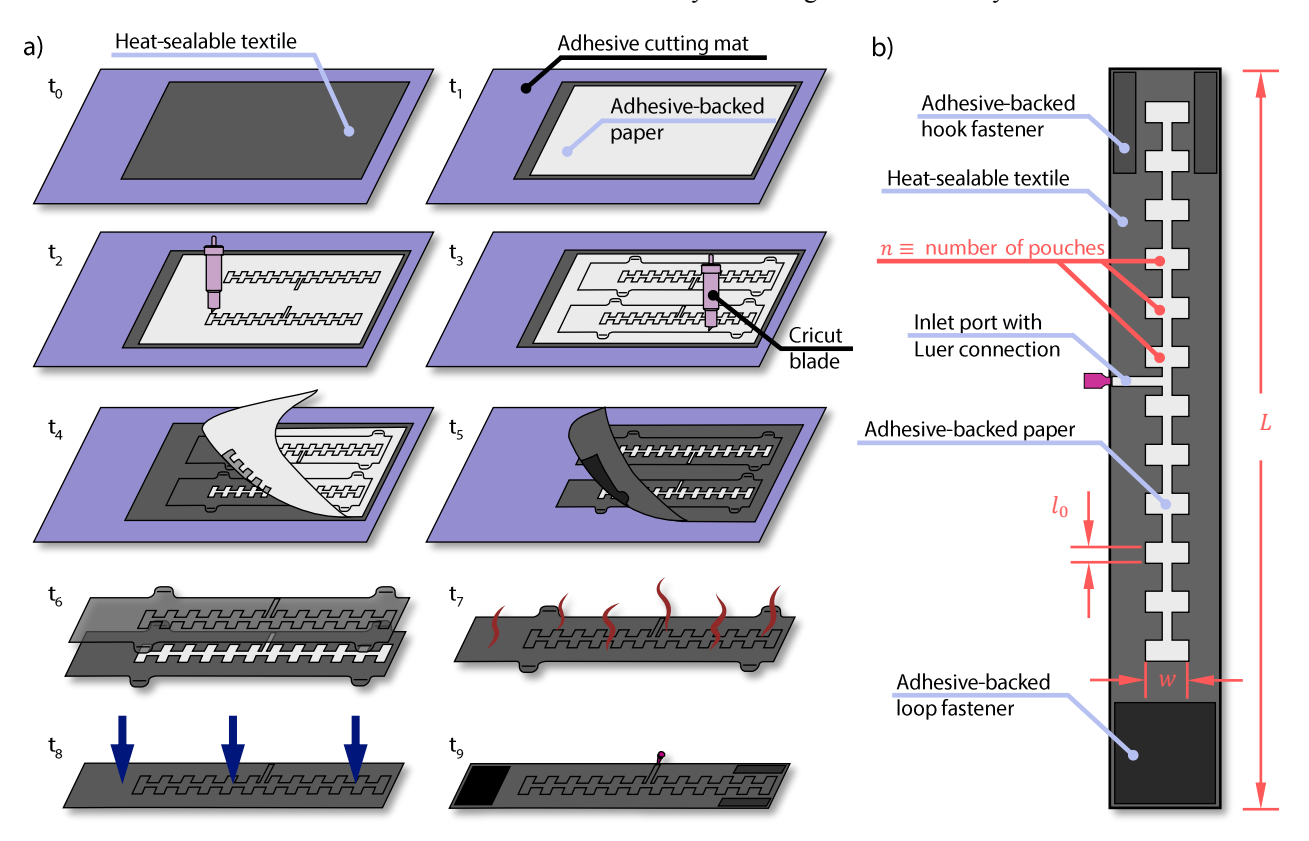


Figure 2. Overview of fabrication and design. (a) Fabrication steps include cutting the heat-sealable textile and non-stick adhesive-backed paper, aligning the mirrored halves, heat pressing, and assembling additional components. (b) Dimensions are shown for pertinent parameters of the squeeze band.

for 30 seconds. Immediately after removal of the pressed layers, we found that it is best to "cold press" the device in a separate pressing machine until the squeeze band fully cools. This process ensures a strong bond between layers of HST and prevents any wrinkles due to uneven contraction during non-isothermal ambient cooling. Features for alignment are trimmed from the squeeze band, and the Luer lock dispensing tip and adhesive-backed hook and loop material are attached.

C. Design

The pouch motor, the basis of our squeeze band, is a well-established mechanism of actuation akin to McKibben actuators [35], [36] and other pneumatic artificial muscles (PAMs) [37], [38]. Defined by the designed internal geometry of the pouches, the squeeze cue (i.e., the induced Laplace pressure from the tangential contraction of serial pouches) is tunable to meet a variety of needs and applications. Discussed more thoroughly in Section III, we varied the internal geometry (e.g., dimensions and aspect ratios) of the pouches and the total number of the pouches, n, to achieve a spectrum of force profiles. The area of each pouch is determined from the pouch width, w, and the pouch length, l_0 (**Fig. 2b**). Varying l_0 , w, and n (and therefore the total active area, $l_0 \times w \times n$) allows for a tunable force response for a given pressure.

The overall device was designed to be approximately the size of a watchband for use on a wrist. The total length, L, is 330 mm; the total width is 50 mm; the distance spanned by all pouches (i.e., the total length of the non-stick layer) was constrained to 250 mm. Accordingly, the dimensions for the internal geometries varied within the millimeter-scale according to dimensional upper limits imposed by a wrist-wearable device and lower limits stemming from the techniques of fabrication.

III. CHARACTERIZATION AND DEMONSTRATION OF A SQUEEZE CUE

A. Experimental Setup

The experimental setup used to characterize our haptic squeeze bands is shown schematically in Fig. 3a. A supply of high pressure from the laboratory's compressed air line was fed into an electronically controlled pressure regulator (8083T1, McMaster-Carr) that was able to regulate the air pressure from 50 kPa to 100 kPa at 10 kPa intervals with an uncertainty of approximately 1 kPa. An accumulator (NY-16, NYAIR) with a volume of 1.89 L was placed downstream of the pressure regulator to act as a pneumatic capacitor. The addition of this tank helped to reduce fluctuations in pressure from downstream activity when inflating the squeeze band. A 3-way, 2-position solenoid valve (VT307, SMC Pneumatics) was electronically controlled to open and close the pneumatic supply to the band. Lastly, just upstream of the squeeze band, a pressure sensor (ADP5151, Panasonic) recorded the actual pressure of the band as it inflated (**Fig. 3b**).

The force generated by the squeeze band was measured endogenously by an ATI Nano25 load cell in an instrumented wrist-shaped test rig. The wrist rig consists of additively manufactured parts (VisiJet-M2R-CL, 3D Systems), acting as a rigid skeletal structure, surrounded by an Eco-Flex silicone

molding (00-30, Smooth-On) that emulates the stiffness of skin.

Before all trials, each band was wrapped around the wrist rig to a preloaded value of 0.5 N. The load cell was zeroed before proceeding with pressurizing the squeeze band and recording experimental data. All force data were filtered through a second-order low-pass Butterworth filter with a critical frequency of 10 Hz and a sampling frequency of 1000 Hz.

B. Static Response

We fabricated six haptic squeeze bands, each with different a combination of pouch lengths (10mm, 15mm, 20mm, or 30mm), pouch widths (20mm or 30mm), and number of pouches (6 or 12 pouches). The dimensions of each design are shown in **Fig. 4a**. An analysis of the steady-state response of the squeeze bands was conducted by attaching each band to the instrumented wrist rig and inflating to a desired pressure. The pressure input for each band ranged from 50 kPa to 100 kPa in 10 kPa intervals; each squeeze band was tested five times at each of these given pressures, and the results of the five trails were averaged for further analysis.

Characteristic trials of the force from each squeeze band at 100 kPa are shown in **Fig. 4b**. The force is primarily dependent on the pouch geometries (l_0 , w) but also depends to a lesser degree on the number of pouches in each squeeze band. A step input of pressure corresponds to a near-step response in force. The rise time, defined as the time required for the force to increase from 10% to 90% of its steady state value, decreases as the pressure increases. The rise time varies from approximately 0.1 seconds to 1 second at 100 kPa of applied pressure depending on the squeeze band's internal geometry.

The squeeze bands demonstrate a wide range of forces across the various pouch parameters. The smallest active area, 10 mm by 20 mm with 6 pouches, has a steady state force of

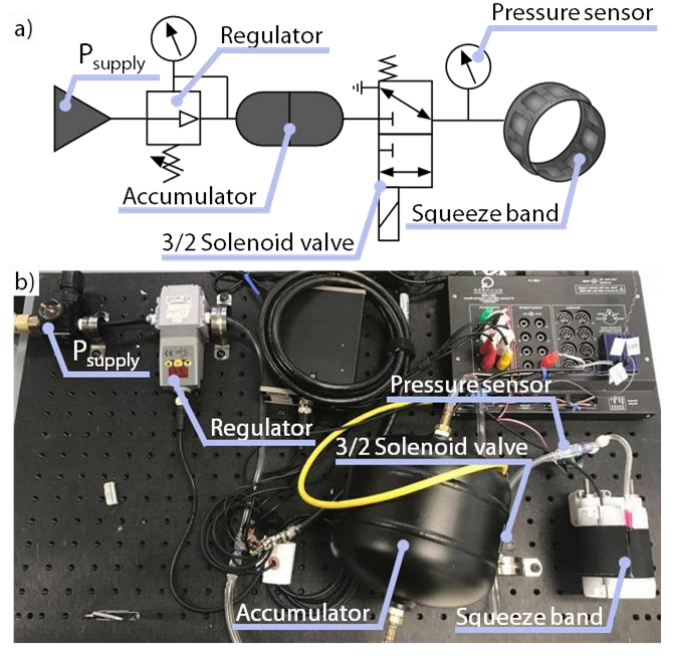


Figure 3. A schematic (a) and photograph (b) depict the experimental setup.

approximately 5 N at 100 kPa of pressure. The largest active area, 30 mm by 30 mm with 6 pouches, exhibits a squeeze force of nearly 70 N at the same applied pressure of 100 kPa. Unlike the other designs, the largest band exhibits a significant fall time likely explained by a kink forming in the channels preventing depressurization when the solenoid is exhausted.

C. Effects of Geometry on the Force Profile

The force-pressure relationships are shown in Fig. 5a for each squeeze band. Each point in the plotted data represents an average of the maximum forces reached over five trials performed for each squeeze band. All squeeze bands, regardless of geometry, show a markedly linear relationship between the force and pressure. This relationship agrees with intuition given that force scales with pressure and area, and area remains approximately the same (upon reaching steady state for a given amount of contraction in a squeeze band). suggesting that force would be directly proportional to the applied pressure. Evidenced by the linear force-pressure trend $(R^2 > 0.98 \text{ for all squeeze bands})$ and the variation in slopes of force versus pressure with a clear dependence on internal geometries, our haptic squeeze bands demonstrate a wide degree of tunability. Our current designs are capable of squeeze forces varying from under 2 N (at 50 kPa) to over 65 N (at 100 kPa). A squeeze band can thus be designed to suit a particular application or user depending on the desired

 $l_0 = 10 \, \text{mm} \ w = 20 \, \text{mm}$ $l_0 = 20 \, \text{mm}$ $w = 20 \,\mathrm{mm}$ $l_0 = 15 \, \text{mm} \ w = 30 \, \text{mm} \ n = 10$ $l_0 = 10 \text{ mm } w = 20 \text{ mm } n = 12$ $l_0 = 30 \, \text{mm}$ $w = 30 \, \text{mm}$ $l_0 = 10 \, \text{mm} \ w = 30 \, \text{mm} \ n = 12$ b) ••• Pressure Normal Force 80 80 1.5 Pressure [bar] Pressure [bar] Normal Force [N] Normal Force [N] 60 60 1 40 40 0.5 0.5 20 20 0 0 0 0 80 80 1.5 Pressure [bar] Pressure [bar] Normal Force [N] Normal Force [N] 60 60 1 1 40 40 0.5 0.5 20 20 0 0 0 0 80 80 1.5 Normal Force [N] Pressure [bar] Pressure [bar] Normal Force [N] 60 60 1 40 40 0.5 20 20 0 0 0 0 0 10 20 0 10 20 Time [s] Time [s]

Figure 4. (a) Parameters of the designs of each squeeze band used in this work. (b) Force responses from a step input pressure of 100 kPa for each squeeze band (solid lines represent normal force; dashed lines represent pressure).

squeeze forces and operating pressures by developing a band with the desired linear force-pressure relationship.

The force output from each squeeze cue was measured in terms of both tangential and normal forces. Tangential forces were calculated from the root sum of squares of the two axes in shear. The magnitudes of tangential and normal forces are shown in **Fig. 5b**. These forces are normalized by the maximum normal force exhibited by each squeeze band, averaged over the 5 trials. The tangential forces remain below 7.5% of the normal forces across all squeeze band designs and applied pressures. The low tangential forces observed in the data indicate that the squeeze band is delivering a squeeze cue without imbuing an additional sensation of a skin-stretch cue, which addresses a limitation of squeeze bands that apply squeeze cues from a single point of contraction (in which the band material must then translate circumferentially [39]).

Furthermore, the apparent self-similarity of normal forces across all of the band designs shown in **Fig. 5b** suggests that an underlying physical model may be applied to describe and optimize performance of our devices in future work.

To demonstrate that our textile-based approach to haptic devices can be seamlessly integrated into everyday wearables, we heat sealed a squeeze band directly onto the sleeve of a standard jersey knit T-shirt (**Fig. 6**). The shirt can be donned

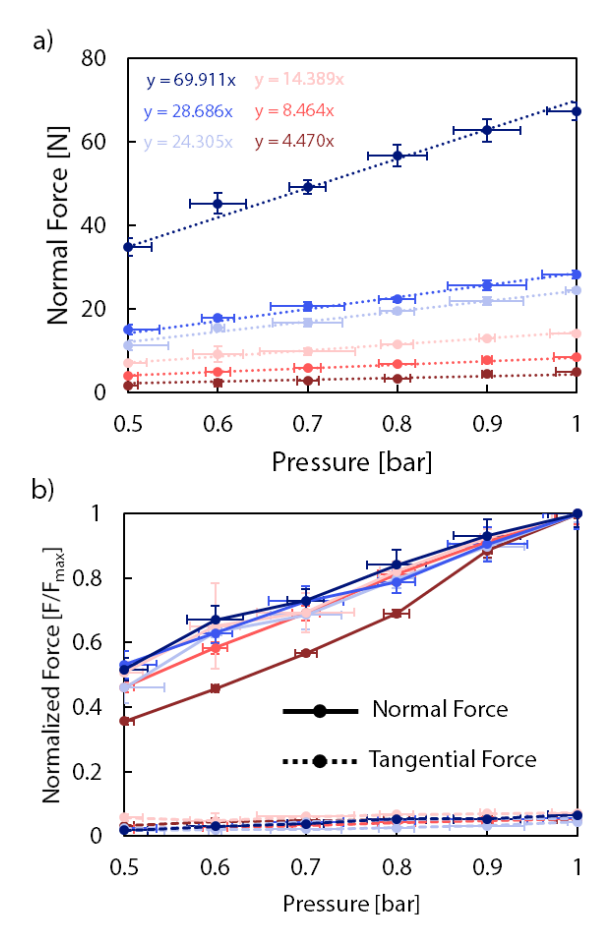


Figure 5. (a) Aggregated force versus pressure response for all types of the squeeze band. (b) Normal and tangential forces normalized to the maximum normal force of each squeeze band. Error bars represent the standard deviation of 5 trials.

and doffed just as one would with a normal shirt. The squeeze band can then be fitted snugly around the arm with hook and loop fastener mounted on an unbonded flap of fabric that extends from the sleeve. This integration showcases one implementation of a variety of designs in which our textile-based haptic squeeze band can be deployed.

IV. CONCLUSION

Our entirely textile-based squeeze band not only offers sufficient forces by leveraging pouch motors that induce Laplace pressure to enact a salient squeeze cue but also exhibits an improvement over existing soft haptic devices by employing a ubiquitous class of materials commonly used in clothing. This work paves the way for well-integrated wearable haptics to become a part of our everyday lives.

The force resulting from a step input of pressure exhibits a step-response output. The forces generated by our haptic squeeze bands are also predominately normal to the wrist (i.e., radial) and thus facilitate a clear squeeze cue. Moreover, as seen from the set of six designs characterized, there exists a wide range of force profiles that are tunable based on both predefined internal geometric designs and real-time adjustment of pressure.

Prior work suggests that a range of 0–10 N is sufficient for squeeze cues [34]. Our squeeze band provides a maximum of 67 N with one version of the squeeze band in the pressures we tested, but the linear force-pressure response of these devices and their broad tunability in terms of range of operating forces suggest that careful design of the internal geometry could generate a haptic squeeze band that varies linearly from 0–10 N for a desired range of input pressures.

The new methodology of design presented here will lead to soft, wearable textile-based haptic devices that are highly tunable and easily integrated into everyday clothing. Interfacing textile-based haptics with soft controllers will be important for harnessing the full set of benefits from such compliant and comfortable devices. While our device currently relies on a simple on-off control scheme, more complex actuation is possible through the addition of control systems and fluidic valves. Many of these components, however, are electromechanical and rigid [40]. Our squeeze band could exhibit a more diverse set of actuation patterns through the employment or integration of a fluidic demultiplexer [41], pneumatic random-access memory storage [42], and a host of soft fluidic logic approaches [43]-[45]. There exists an abundance of future directions for integrated control of a fully soft squeeze band; future work could explore the intersection of textile-based haptics with soft controllers.

REFERENCES

- [1] M. K. O'Malley and A. Gupta, "Haptic Interfaces," in HCI Beyond the GUI, Elsevier, 2008, pp. 25–73. doi: 10.1016/B978-0-12-374017-5.00002-X.
- [2] J. L. Sullivan et al., "Multi-Sensory Stimuli Improve Distinguishability of Cutaneous Haptic Cues," *IEEE Transactions on Haptics*, vol. 13, no. 2, pp. 286–297, Apr. 2020, doi: 10.1109/TOH.2019.2922901.
- [3] E. Pezent et al., "Explorations of Wrist Haptic Feedback for AR/VR Interactions with Tasbi," in Extended Abstracts of the 2020 CHI



Figure 6. Seamless integration of a textile-based haptic device into a garment. (a) Shirt with a squeeze-enabled haptic device permanently heat sealed onto the sleeve. (b) Hook and loop fastening method to tighten the sleeve around the arm for a salient cue. (c) Unpressurized squeeze band on arm. (d) Squeeze cue delivered through application of pressurized air.

Conference on Human Factors in Computing Systems, New York, NY, USA, Apr. 2020, pp. 1–4. doi: 10.1145/3334480.3383151.

- [4] F. Chinello, C. Pacchierotti, J. Bimbo, N. G. Tsagarakis, and D. Prattichizzo, "Design and Evaluation of a Wearable Skin Stretch Device for Haptic Guidance," *IEEE Robotics and Automation Letters*, vol. 3, no. 1, pp. 524–531, Jan. 2018, doi: 10.1109/LRA.2017.2766244.
- [5] J. D. Brown, J. N. Fernandez, S. P. Cohen, and K. J. Kuchenbecker, "A Wrist-Squeezing Force-Feedback System for Robotic Surgery Training," in 2017 IEEE World Haptics Conference (WHC), Jun. 2017, pp. 107–112. doi: 10.1109/WHC.2017.7989885.
- [6] E. Treadway, B. Gillespie, D. Bolger, A. Blank, M. K. O'Malley, and A. Davis, "The Role of Auxiliary and Referred Haptic Feedback in Myoelectric Control," in 2015 IEEE World Haptics Conference (WHC), Jun. 2015, pp. 13–18. doi: 10.1109/WHC.2015.7177684.
- [7] P. B. Shull and D. D. Damian, "Haptic Wearables as Sensory Replacement, Sensory Augmentation and Trainer – A Review," *J NeuroEngineering Rehabil*, vol. 12, no. 1, p. 59, Jul. 2015, doi: 10.1186/s12984-015-0055-z.
- [8] C. Pacchierotti, S. Sinclair, M. Solazzi, A. Frisoli, V. Hayward, and D. Prattichizzo, "Wearable Haptic Systems for the Fingertip and the Hand: Taxonomy, Review, and Perspectives," *IEEE Transactions on Haptics*, vol. 10, no. 4, pp. 580–600, Oct. 2017, doi: 10.1109/TOH.2017.2689006.

- [9] S. Song, G. Noh, J. Yoo, I. Oakley, J. Cho, and A. Bianchi, "Hot & Tight: Exploring Thermo and Squeeze Cues Recognition on Wrist Wearables," in *Proceedings of the 2015 ACM International Symposium on Wearable Computers*, New York, NY, USA, Sep. 2015, pp. 39–42. doi: 10.1145/2802083.2802092.
- [10] A. A. Stanley and K. J. Kuchenbecker, "Evaluation of Tactile Feedback Methods for Wrist Rotation Guidance," *IEEE Transactions* on *Haptics*, vol. 5, no. 3, pp. 240–251, 2012, doi: 10.1109/TOH.2012.33.
- [11] C. V. Keef et al., "Virtual Texture Generated Using Elastomeric Conductive Block Copolymer in a Wireless Multimodal Haptic Glove," Advanced Intelligent Systems, vol. 2, no. 4, p. 2000018, 2020, doi: 10.1002/aisy.202000018.
- [12] A. Delazio, K. Nakagaki, R. L. Klatzky, S. E. Hudson, J. F. Lehman, and A. P. Sample, "Force Jacket: Pneumatically-Actuated Jacket for Embodied Haptic Experiences," in *Proceedings of the 2018 CHI Conference on Human Factors in Computing Systems*, New York, NY, USA: Association for Computing Machinery, 2018, pp. 1–12. doi: 10.1145/3173574.3173894
- [13] C. Rognon, M. Koehler, C. Duriez, D. Floreano, and A. M. Okamura, "Soft Haptic Device to Render the Sensation of Flying Like a Drone," *IEEE Robotics and Automation Letters*, vol. 4, no. 3, pp. 2524–2531, Jul. 2019, doi: 10.1109/LRA.2019.2907432.
- [14] E. Kitamura, H. Nabae, G. Endo, and K. Suzumori, "Self-Excitation Pneumatic Soft Actuator Inspired by Vocal Cords," Sensors and Actuators A: Physical, vol. 331, p. 112816, Nov. 2021, doi: 10.1016/j.sna.2021.112816.
- [15] R. H. Heisser et al., "Valveless Microliter Combustion for Densely Packed Arrays of Powerful Soft Actuators," PNAS, vol. 118, no. 39, Sep. 2021, doi: 10.1073/pnas.2106553118.
- [16] A. Marette, A. Poulin, N. Besse, S. Rosset, D. Briand, and H. Shea, "Flexible Zinc–Tin Oxide Thin Film Transistors Operating at 1 kV for Integrated Switching of Dielectric Elastomer Actuators Arrays," *Advanced Materials*, vol. 29, no. 30, p. 1700880, 2017, doi: 10.1002/adma.201700880.
- [17] H. Phung et al., "Interactive Haptic Display Based on Soft Actuator and Soft Sensor," in 2017 IEEE/RSJ International Conference on Intelligent Robots and Systems (IROS), Sep. 2017, pp. 886–891. doi: 10.1109/IROS.2017.8202250.
- [18] M. Zhu, T. N. Do, E. Hawkes, and Y. Visell, "Fluidic Fabric Muscle Sheets for Wearable and Soft Robotics," *Soft Robotics*, vol. 7, no. 2, pp. 179–197, Apr. 2020, doi: 10.1089/soro.2019.0033.
- [19] M. Zhu et al., "PneuSleeve: In-fabric Multimodal Actuation and Sensing in a Soft, Compact, and Expressive Haptic Sleeve," in Proceedings of the 2020 CHI Conference on Human Factors in Computing Systems, Honolulu HI USA, Apr. 2020, pp. 1–12. doi: 10.1145/3313831.3376333.
- [20] A. Akther, J. O. Castro, S. A. M. Shaegh, A. R. Rezk, and L. Y. Yeo, "Miniaturised Acoustofluidic Tactile Haptic Actuator," *Soft Matter*, vol. 15, no. 20, pp. 4146–4152, 2019, doi: 10.1039/C9SM00479C.
- [21] W. Wu and H. Culbertson, "Wearable Haptic Pneumatic Device for Creating the Illusion of Lateral Motion on the Arm," in 2019 IEEE World Haptics Conference (WHC), Jul. 2019, pp. 193–198. doi: 10.1109/WHC.2019.8816170.
- [22] E. M. Young, A. H. Memar, P. Agarwal, and N. Colonnese, "Bellowband: A Pneumatic Wristband for Delivering Local Pressure and Vibration," in 2019 IEEE World Haptics Conference (WHC), Jul. 2019, pp. 55–60. doi: 10.1109/WHC.2019.8816075.
- [23] R. Niiyama, D. Rus, and S. Kim, "Pouch Motors: Printable/Inflatable Soft Actuators for Robotics," in 2014 IEEE International Conference on Robotics and Automation (ICRA), May 2014, pp. 6332–6337. doi: 10.1109/ICRA.2014.6907793.
- [24] A. R. Mettam, "Inflatable Servo Actuators," Aeronautical Research Council, Ministry of Aviation, C. P. No. 671, 1962.
- [25] P.-G. de Gennes, F. Brochard-Wyart, and D. Quéré, "Capillarity: Deformable Interfaces," in *Capillarity and Wetting Phenomena: Drops, Bubbles, Pearls, Waves*, P.-G. de Gennes, F. Brochard-Wyart, and D. Quéré, Eds. New York, NY: Springer, 2004, pp. 1–31. doi: 10.1007/978-0-387-21656-0 1.
- [26] D. T. Goetz, D. K. Owusu-Antwi, and H. Culbertson, "PATCH: Pump-Actuated Thermal Compression Haptics," in 2020 IEEE

- Haptics Symposium (HAPTICS), Mar. 2020, pp. 643–649. doi: 10.1109/HAPTICS45997.2020.ras.HAP20.32.c4048ec3.
- [27] H. Pohl, P. Brandes, H. Ngo Quang, and M. Rohs, "Squeezeback: Pneumatic Compression for Notifications," in *Proceedings of the* 2017 CHI Conference on Human Factors in Computing Systems, Denver Colorado USA, May 2017, pp. 5318–5330. doi: 10.1145/3025453.3025526.
- [28] T. Mitsuda, "Pseudo Force Display that Applies Pressure to the Forearms," Presence: Teleoperators and Virtual Environments, vol. 22, no. 3, pp. 191–201, Aug. 2013, doi: 10.1162/PRES_a_00150.
- [29] C. Tejeiro, C. E. Stepp, M. Malhotra, E. Rombokas, and Y. Matsuoka, "Comparison of Remote Pressure and Vibrotactile Feedback for Prosthetic Hand Control," in 2012 4th IEEE RAS EMBS International Conference on Biomedical Robotics and Biomechatronics (BioRob), Jun. 2012, pp. 521–525. doi: 10.1109/BioRob.2012.6290268.
- [30] C. Vaucelle, L. Bonanni, and H. Ishii, "Design of Haptic Interfaces for Therapy," in *Proceedings of the SIGCHI Conference on Human Factors in Computing Systems*, New York, NY, USA, Apr. 2009, pp. 467–470. doi: 10.1145/1518701.1518776.
- [31] V. Sanchez et al., "Smart Thermally Actuating Textiles," Advanced Materials Technologies, vol. 5, no. 8, p. 2000383, Aug. 2020, doi: 10.1002/admt.202000383
- [32] B. Jumet, M. D. Bell, V. Sanchez, and D. J. Preston, "A Data-Driven Review of Soft Robotics," *Advanced Intelligent Systems*, vol. n/a, no. n/a, p. 2100163, doi: 10.1002/aisy.202100163.
- [33] V. Sanchez, C. J. Walsh, and R. J. Wood, "Textile Technology for Soft Robotic and Autonomous Garments," *Advanced Functional Materials*, vol. 31, no. 6, p. 2008278, 2021, doi: 10.1002/adfm.202008278.
- [34] E. Pezent, P. Agarwal, J. Hartcher-O'Brien, N. Colonnese, and M. K. O'Malley, "Design, Control, and Psychophysics of Tasbi: A Force-Controlled Multimodal Haptic Bracelet," *IEEE Transactions on Robotics*, in press.
- [35] A. A. Mohd Faudzi, G. Endo, S. Kurumaya, and K. Suzumori, "Long-Legged Hexapod Giacometti Robot Using Thin Soft McKibben Actuator," *IEEE Robotics and Automation Letters*, vol. 3, no. 1, pp. 100–107, Jan. 2018, doi: 10.1109/LRA.2017.2734244.
- [36] A. A. M. Faudzi, M. R. M. Razif, G. Endo, H. Nabae, and K. Suzumori, "Soft-Amphibious Robot Using Thin and Soft McKibben Actuator," in 2017 IEEE International Conference on Advanced Intelligent Mechatronics (AIM), Jul. 2017, pp. 981–986. doi: 10.1109/AIM.2017.8014146.
- [37] D. Yang et al., "Buckling Pneumatic Linear Actuators Inspired by Muscle," Advanced Materials Technologies, vol. 1, no. 3, p. 1600055, 2016, doi: 10.1002/admt.201600055.
- [38] S. Sanan, P. S. Lynn, and S. T. Griffith, "Pneumatic Torsional Actuators for Inflatable Robots," *Journal of Mechanisms and Robotics*, vol. 6, no. 3, Apr. 2014, doi: 10.1115/1.4026629.
- [39] E. Pezent et al., "Tasbi: Multisensory Squeeze and Vibrotactile Wrist Haptics for Augmented and Virtual Reality," in 2019 IEEE World Haptics Conference (WHC), Jul. 2019, pp. 1–6. doi: 10.1109/WHC.2019.8816098.
- [40] A. Rajappan, B. Jumet, and D. J. Preston, "Pneumatic Soft Robots Take a Step Toward Autonomy," *Science Robotics*, vol. 6, no. 51, Feb. 2021, doi: 10.1126/scirobotics.abg6994.
- [41] N. W. Bartlett, K. P. Becker, and R. J. Wood, "A Fluidic Demultiplexer for Controlling Large Arrays of Soft Actuators," Soft Matter, vol. 16, no. 25, pp. 5871–5877, Jul. 2020, doi: 10.1039/C9SM02502B.
- [42] S. Hoang, K. Karydis, P. Brisk, and W. H. Grover, "A Pneumatic Random-Access Memory for Controlling Soft Robots," *PLOS ONE*, vol. 16, no. 7, p. e0254524, Jul. 2021, doi: 10.1371/journal.pone.0254524.
- [43] D. J. Preston et al., "Digital Logic for Soft Devices," Proceedings of the National Academy of Sciences, vol. 116, no. 16, pp. 7750–7759, Apr. 2019, doi: 10.1073/pnas.1820672116.
- [44] P. Rothemund *et al.*, "A Soft, Bistable Valve for Autonomous Control of Soft Actuators," *Science Robotics*, vol. 3, no. 16, p. eaar7986, Mar. 2018, doi: 10.1126/scirobotics.aar7986.
- [45] D. J. Preston et al., "A Soft Ring Oscillator," Science Robotics, vol. 4, no. 31, Jun. 2019, doi: 10.1126/scirobotics.aaw5496.